Comparison of HPLC and Stereologic Image Analysis for the Quantitation of Eu- and Pheomelanins in Nevus Cells and Stimulated Melanoma Cells[1]

Eric Donois, Véronique del Marmol,* Ghanem Ghanem,* and Jean-Étienne Surlève-Bazeille

Defense and Cell Regulation Factors, Animal Biology Institute, Talence, France; *Laboratory of Oncology and Experimental Surgery (LOCE), Jules Bordet Institute, Bruxelles, Belgium

The aim of the study was to compare two methods of quantitating eumelanins and pheomelanins, pigments synthesized by melanocytes. One is based on the high performance liquid chromatography quantitation of specific degradation products of each melanin type. The other requires image analysis, transmission electron microscopy, and stereology. In a previous study, we showed good correlations between both methods for total melanin but not for eumelanins or pheomelanins. We describe here the same comparison in more pigmented cells (nevus cells and stimulated HBL melanoma cells). Transmission electron microscopy micrographs were image analyzed to generate several primary parameters. Stereology was used for estimating melanosomal maturation, intracellular melanin content, and the number of melanized melanosomes per cell, for total melanin, eumelanins, or pheomelanins. Our results showed a good correlation between both methods for total melanin, eumelanins, and pheomelanins with an r equal to 0.99, 0.91, and 0.93, respectively, when all the points were used in the linear regression analyses. In the melanoma cell group (HBL cells cultured in media of different compositions), the chemical and morphometric estimations were not parallel in the case of eumelanins and pheomelanins. In addition, the stereologic and high performance liquid chromatography pheomelanins to eumelanins ratios were still not correlated. These results demonstrate the relevancy of the stereologic method, but the low level of melanization, the possible lack of specificity of melanogenesis in melanoma cells, and a problem of sensitivity of the stereologic method in this context seem to be obstacles in obtaining better results. The utilization of normal human melanocytes could give some answers to our hypotheses. ***Key words: alkali elution/morphometry/normal epidermal melanocytes/transmission electron microscopy. J Invest Dermatol 111:422–428, 1998***

Melanocytes are pigment producing cells originating in the neural crest that migrate to several organs during embryogenesis, and particularly to the dermo–epidermal junction and to hair follicles in mammals (Rawles, 1947; Wehrle-Haller *et al*, 1996). Two distinct types of pigment, eumelanins and pheomelanins, which are black-brown and yellow-reddish, respectively (Prota, 1980), can be synthesized by melanocytes in specialized organelles named melanosomes. In mammals, typical eumelanosomes are elliptic and lamellar (fibrillar) and pheomelanosomes are spherical with a spotty pattern of melanin deposition (Jimbow *et al*, 1983; Inazu and Mishima, 1993; Ortonne and Prota, 1993; Schraermeyer, 1996). Pheomelanins and eumelanins have been chemically identified and quantitated in human epidermis by high performance liquid chromatography (HPLC) (Thody *et al*, 1991; Hunt *et al*, 1995a), but the structure–function relationship of eumelanosomes and pheomelanosomes is better described in mouse and mammalian hair (Jimbow *et al*, 1983; Ortonne and Prota, 1993).

Inside melanosomes, eumelanogenesis and pheomelanogenesis begin by the conversion of L-tyrosine (L-Tyr) to L-3,4-dihydroxyphenylalanine (L-DOPA), which undergoes oxidation to DOPAquinone. Recent studies, however, have shown that L-DOPA is probably not an actual intermediate in mammalian melanogenesis and that L-Tyr undergoes a direct transformation to DOPAquinone intermediates.[2,3] The melanosomal enzyme involved in these stages is tyrosinase (Prota, 1993). After these two common stages, eumelanogenesis and pheomelanogenesis separate: DOPAquinone may be converted into either DOPAchrome or cysteinylDOPA (involvement of cysteine and/or glutathione), initial stages of the eumelanogenic and pheomelanogenic pathways,

Manuscript received December 4, 1997; revised May 12, 1998; accepted for publication May 18, 1998.

Reprint requests to: Dr. E. Donois, Defense and Cell Regulation Factors, Animal Biology Institute, Avenue des Facultés, 33405 Talence, France.

Abbreviations: DHI, 5,6-dihydroxyindole; DHICA, 5,6-dihydroxyindole-2-carboxylic acid; MVC, mean variation coefficient; P/E ratio, pheomelanin to eumelanin ratio; Tyr, tyrosine.

[1]This work was partially presented at the Fifth Congress of the International Society for Skin Imaging, Vienna, Austria, September 1997, and the Seventh Annual Meeting of the European Society for Pigment Cell Research, Bordeaux, France, October 1997.

[2]Riley PA, Cooksey CJ, Land EJ, Pavel S, Ramsden CA, Smit NPM: The mechanism of tyrosinase auto-activation. Part 1: oximetric studies of kinetics and stochiometry of N-substituted mono-and dihydric phenol substrates. Seventh Meeting of the European Society for Pigment Cell Research, Bordeaux, France, October 9–11 1997. *Pigment Cell Res* 10:349, 1997 (abstr.)

[3]Land EJ, Cooksey CJ, Pavel S, Ramsden CA, Riley PA, Smit NPM: The mechanism of tyrosinase auto-activation. Part 2: pulse radiolysis studies of N,Ndialkyldopaquinone cyclization to form novel indoliumolates. Seventh Meeting of the European Society for Pigment Cell Research, Bordeaux, France, October 9–11 1997. *Pigment Cell Res* 10:349, 1997 (abstr.)

respectively (Ito, 1993; del Marmol *et al*, 1996). DOPAchrome tautomerase (tyrosinase-related protein-2) converts DOPAchrome to 5,6-dihydroxyindole-2-carboxylic acid (DHICA; Leonard *et al*, 1988; Kameyama *et al*, 1993; Solano *et al*, 1996), but DOPAchrome also gives 5,6-dihydroxyindole (DHI). Tyrosinase-related protein-1, which is associated with eumelanogenesis (del Marmol *et al*, 1993), catalyzes the oxidation of DHICA to eumelanin oligomers (Jiménez-Cervantes *et al*, 1994; Kobayashi *et al*, 1994). Finally, eumelanins are formed by the copolymerization of variable proportions of DHI and DHICA (Odh *et al*, 1994; Ozeki *et al*, 1995). In pheomelanogenesis, cysteinyl-DOPA forms benzothiazine derivatives that polymerize into pheomelanin (Prota, 1980; Napolitano *et al*, 1996).

The best chemical method for quantitating eumelanins and pheomelanins requires the solubilization, the degradation of melanins and the measurement of specific degradation products by HPLC. Even though this method has proved very useful in the understanding of the regulation of the composition of the intracellular melanin content, it remains indirect because it quantifies specific degradation products and reflects a global chemical composition in each type of monomer in melanins, but also in low molecular weight oligomers not deposited as melanin particles. Recently, we developed a stereologic image analysis method allowing the estimation of various intracellular and intramelanosomal melanization parameters (Donois *et al*, 1997).[4] This method is more direct because it quantifies melanins in their polymeric state and preserves the three-dimensional structure of the pigment inside melanosomes without any extraction or solubilization (i.e., depolymerization). Several aspects of this approach were improved thus making it possible to conceive the analysis of poorly pigmented cells, to analyze mixed cell populations (melanocytes and keratinocytes for instance), and to quantitate eumelanins and pheomelanins (Donois *et al*, 1998a). More recently, we utilized six human melanoma cell lines in order to compare stereology and HPLC in quantitating eumelanins and pheomelanins (Donois *et al*, 1998b). Although total melanin stereologic data were correlated with HPLC data, eumelanins and pheomelanins data were not correlated. This led us to formulate several hypotheses, the main one being the effect of the very low melanization level in these cells on the quality of stereologic estimators.

In this study, similar HPLC *versus* stereology comparisons were performed in two highly pigmented nevus cell lines and one melanoma cell line cultured in four culture conditions favoring melanogenesis. We obtained good correlations between HPLC and stereology for total melanin, eumelanins, and pheomelanins but not for the pheomelanin to eumelanin (P/E) ratio. Nevertheless, when considering only melanoma cells, even stimulated, we did not observe any correlation for eumelanin and pheomelanin data; this suggests that our stereologic method is perhaps more suited to normal epidermal melanocytes. These encouraging results have now to be clarified, reproduced, or improved in normal human epidermal melanocytes.

MATERIALS AND METHODS

Melanocytic cells HBL are human melanoma cells established in the Laboratory of Oncology and Experimental Surgery (LOCE) (del Marmol *et al*, 1993) and LEA and CARA are two nevus cell lines established in the same laboratory. These cells were cultured at the LOCE in standard Ham F10 medium (10 μM Tyr and 206 μM cysteine) supplemented with 10% fetal calf serum, 1% of a penicillin–streptomycin mixture containing 10,000 U per ml and 10,000 μg per ml, respectively, 1% of kanamycin (1000 μg per ml) and 1% of a 200 mM glutamine solution. Cells were seeded at 6×10^6 per 175 cm^2 flask. HBL melanoma cells were cultured either in 40 μM Tyr/20.6 μM cysteine medium or in 40 μM Tyr/206 μM cysteine medium for three passages. After the fourth passage the number of experimental conditions was multiplied by two for 3 d of culture by addition of a new Tyr concentration (110 μM), allowing four conditions in HBL cells. The 40 μM Tyr/206 μM cysteine condition, however, was excluded from the linear regression analyses because of the unnecessary redundancy of this point. HBL cells cultured in Tyr-enriched Ham F10 medium (110 μM Tyr and 206 μM cysteine) for 39 passages were also used. We thus obtained six experimental points for our linear regression analyses (four points for HBL melanoma cells and two points for the nevus cells of the LEA and CARA lines).

Table I.

	Vv(mi,cy) (without unit)	V(mi,ce) (μm^3)	n″(m,ce) ($cell^{-1}$)	a(mi,m) (μm^2)
Description	Cytoplasmic volume density of melanin	Melanin volume per average cell	Number of melanized melanosomes per average cell	Mean melanin area per melanized melanosome profile (melanosomal maturation)

Fixation and embedding Melanocytic cells were fixed in suspension. This technique was specifically elaborated in order to obtain near spherical to spherical melanocytes and to embed them as pellets (Donois *et al*, 1997). Briefly, melanocytic cells were detached, pelleted, washed, and fixed in suspension with glutaraldehyde after leaving the cell suspension in cacodylate buffer for 20 min as previously described (Donois *et al*, 1997). After the osmium tetroxide fixation (Donois *et al*, 1997), an ethanol dehydration was performed, followed by an infiltration with absolute ethanol:1,2-epoxypropane (1:1 vol/vol, 15 min), 1,2-epoxypropane (15 min), 1,2-epoxypropane:complete embedding medium (1:1 vol/vol, overnight). The cell suspension was homogenized and sampled in pyramidal tipped plastic capsules (Beem). The preceding solution was replaced by complete embedding medium (Epon) after the last centrifugation.

It is essential to obtain pellets of spherical cells to estimate easily the cellular volume, which is a very important parameter, and to obtain good quality samples (ultrathin sections) of the cell population after embedding (Donois *et al*, 1997). Embedded cell pellets were cut into eight roughly equal size pieces: four from the summit (S) and four from the base (B) of the pyramidal pellet. Then, one S piece and one B piece were finally randomly selected among the eight pieces and haphazardly re-embedded in Epon. The resulting blocks were routinely cut in the center of each re-embedded piece, one perfect section per block was observed and 20 melanocyte profiles per section were image analyzed (see Donois *et al*, 1998b, for details).

Transmission electron microscopy Seventy nanometer-thick ultrathin sections were cut with a Ultracut S ultramicrotome (Reichert-Jung) equipped with a diamond knife (Diatome). Sections were submitted to chloroform vapor to correct possible deformations due to compression (Bron *et al*, 1990). Sections were collected with 150 mesh copper grids, stained with 2% uranyl acetate in 50% ethanol, and poststained with 0.2% lead citrate. Sections were observed with a Jeol 1200-EX transmission electron microscope under an accelerating voltage of 80 kV. Micrographs of calibration grids (2160 lines per mm carbon grating replicas) were used for calibration of our image analysis system (Poole, 1992).

Alkali elution of pheomelanins on ultrathin sections The alkali elution method (Mishima, 1990; Inazu and Mishima, 1993) was modified as follows: each grid supporting ultrathin sections was deposited on a drop of 300 mM sodium hydroxide (NaOH) for 45 min and rinsed with bi-distilled water before staining. This technique proved specific in dissolving pheomelanins in human follicular melanocytes (Donois *et al*, 1998a).

Image analysis and stereology Micrographs were digitized with an Agfa Color scanner (Agfa, Mortsel, Belgium) and stored on a hard disk at eight bits per square pixel and 256 gray levels. A digitization resolution of 100 dots per inch of micrograph was used. The Semper 6 Plus image analysis software (Synoptics, Cambridge, U.K.) was used to execute our Quantimel program, enabling us to extract and measure melanin profiles and to estimate the following primary data: A_n, nuclear area; A_{ce}, cell area; A_{mi}, melanin area; N_{mp}, number of melanin particles; N_{co}, number of connections between melanin particles (Donois *et al*, 1997). Melanin was gray level thresholded according to the SEM method by using the SEM2 threshold (Donois *et al*, 1998a). This thresholding technique is based on a computer-assisted systematic-random sampling of the mean peripheral melanin gray levels.

The primary data obtained by image analysis were used in stereology to calculate stereologic three-dimensional melanization parameters (Weibel, 1979, 1989; Mayhew and White, 1980; Bolender, 1992; Donois *et al*, 1997). The three-dimensional melanization parameters are described in **Table I**: briefly, v(mi,ce) is the eumelanin, pheomelanin, or total melanin volume per average cell; VV(mi,cy) is the cytoplasmic volume density of eumelanin, pheomelanin,

[4]Donois E, Surlève-Bazeille J-E, Taïeb A: Quantitative stereological image analysis of human cultured melanocytes observed by transmission electron microscopy. Fifth Meeting of the European Society for Pigment Cell Research, Vienna, Austria, October 1994. *Melanoma Res* 4:18, 1994 (abstr.)

or total melanin; n″(m,ce) is the best estimator of the number of melanized melanosomes per average cell for eumelanin, pheomelanin, or total melanin; and a(mi,m) is the eumelanin, pheomelanin, or total melanin area per average melanized melanosome profile. These parameters were chosen in a preliminary study (Donois *et al*, 1997) because they are either unbiased [VV(mi,cy) and v(mi,ce)] or biased with a constant bias [n″(m,ce) and a(mi,m)]. Because their bias can be considered as constant, n″(m,ce) and a(mi,m) can then be used for quantitative comparisons.

Conventionally stained sections were used for the estimation of total melanin parameters and the primary data obtained were summed over 20 melanocyte profiles (for each of the S and B blocks) before stereologic calculations. For the estimation of eumelanins, the same was performed with alkali-treated sections when for pheomelanins, eumelanins primary data summed over 20 melanocyte profiles from the S or B blocks where subtracted to the corresponding summed primary data obtained for total melanin. Finally, for each pigment and for each parameter, the mean between S and B values (m), the SD, and the variation coefficient [VC(%) = SD/m × (100)] were calculated.

The P/E ratio was calculated by using VV(mi,cy), n″(m,ce), A(mi,cp) (melanin area per average cell profile), or N(m,cp) (number of melanized melanosomes per average cell profile), and for each of these possibilities, two estimators could be calculated: the mean of the P/E ratios obtained in the S and B blocks or the P/E ratio calculated by averaging P and E over S and B.

Estimation of mean cell volume For each condition, 30 cells were systematically sampled in a Malassez cell and measured at the rinsing stage of the osmium tetroxide postfixation with a calibrated optical microscope, equipped with an eyepiece micrometer. For some nonspherical cells (10%–20%), ellipsoidal shape was assumed and the formula $D_{VES} = (D_1^2 \times D_2)^{1/3}$ was used, where D_1 is the long axis diameter, D_2 is the short axis diameter, and D_{VES} is the diameter of the volume-equivalent sphere. This estimation was done in duplicate and the mean cell diameter (MCD) was used to calculate v_{ce} (cell volume) according to the formula $v_{ce} = \pi(MCD)^3/6$. The cell volume is particularly essential to estimate v(mi,ce) and n″(m,ce) (Donois *et al*, 1997).

HPLC determination of eumelanins and pheomelanins in melanocytic cells The concentration of eumelanins and pheomelanins in extracts of 10^6 cells were determined by HPLC at the LOCE according to the method extensively described elsewhere (Ito and Fujita, 1985; Ito, 1993; Ito and Wakamatsu, 1994). Briefly, permanganate oxidation of eumelanins to pyrrole-2,3,5-tricarboxylic acid and hydriodic acid hydrolysis of pheomelanins to aminohydroxyphenylalanine were used to estimate pigment content. Total melanin amount was estimated by 50 × pyrrole-2,3,5-tricarboxylic acid + 5 × aminohydroxyphenylalanine (μg per 10^6 cells) according to the known chemical degradation yields of eumelanins and pheomelanins (Ito and Jimbow, 1983; Ito, 1993; Ito and Wakamatsu, 1994). Linear regression analyses between HPLC and stereologic data were performed by using the y = ax model except for P/E ratios for which the y = ax + b model was also used. Several data are given as mean ± SD.

Linear regression analyses concerning total melanin, eumelanins, and pheomelanins HPLC and stereologic data were either performed for all the cell lines and experimental conditions (six points) or for HBL cells alone (four points corresponding to four different culture media compositions described in *Melanocytic cells*). The same could not be performed in nevus cells because we only had two nevus cell lines at our disposal. These analyses were accomplished in order to test several hypotheses emitted at the end of our preceding study (Donois *et al*, 1998b).

The correlation coefficient (r) was calculated according to the Bravais–Pearson's formula. The gaussian distribution of the variables studied was assumed in order to test the significance of r at p = 0.05 with the corresponding parametric test. The gaussian distribution being unverifiable, due to the low number of measurements, we also used a nonparametric Kendall's test. For increased clarity, the results of the statistical assessment of the significance of the correlations are given in the *Discussion*.

RESULTS

Stereologic data The variability of total melanin stereologic estimators was satisfactory because the mean variation coefficient (MVC) was 22.42%, 14.64%, and 9% in the case of v(mi,ce) (**Fig 1*A***), n″(m,ce) (not shown), and a(mi,m) (**Fig 1*B***), respectively. These variabilities in total melanin stereologic data represent better results than in our previous study (Donois *et al*, 1998b).

For eumelanins, the MVC was equal to 42.26% (**Fig 2*A***), 47.34%, and 16.38% (**Fig 2*B***) in the case of v(mi,ce), n″(m,ce) (not shown), and a(mi,m), respectively. These MVC values remain acceptable and far less than those achieved in our previous study for the same pigment

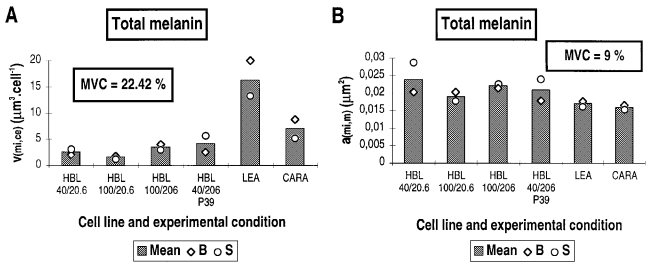

Figure 1. Volume of total melanin per average cell (*A*), the corresponding melanosomal maturation (*B*), and associated MVC for the different experimental conditions and cell lines. B and S, base and summit of the original pyramidal cell pellet (see *Materials and Methods*).

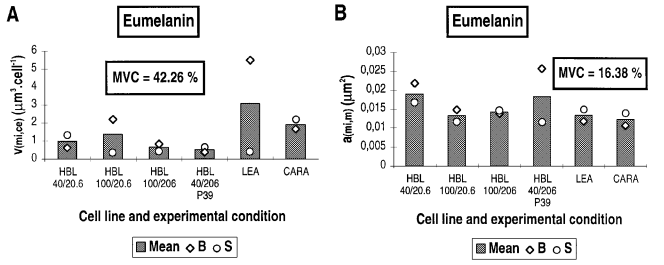

Figure 2. Volume of eumelanin per average cell (*A*), the corresponding melanosomal maturation (*B*), and associated MVC for the different experimental conditions and cell lines. B and S, base and summit of the original pyramidal cell pellet (see *Materials and Methods*).

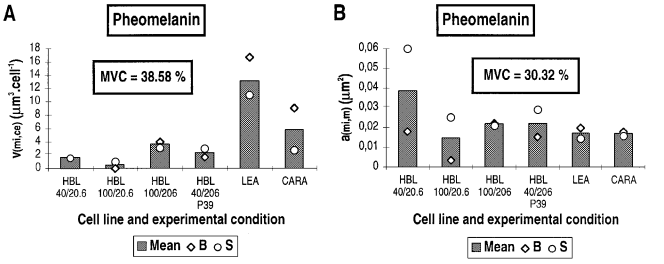

Figure 3. Volume of pheomelanin per average cell (*A*), the corresponding melanosomal maturation (*B*), and associated MVC for the different experimental conditions and cell lines. B and S, base and summit of the original pyramidal cell pellet (see *Materials and Methods*).

(Donois *et al*, 1998b), because the MVC was almost equal to 70% for v(mi,ce).

When considering pheomelanins, variabilities were close to those calculated for eumelanin stereologic data because the MVC was 38.58% (**Fig 3*A***), 40.85%, and 30.32% (**Fig 3*B***) for v(mi,ce), n″(m,ce) (not shown), and a(mi,m), respectively. These variabilities are comparable with those obtained in our previous study for the same pigment (Donois *et al*, 1998b).

Comparison of HPLC and stereologic data by linear regression analysis

All cell lines and experimental conditions v(mi,ce) and n″(m,ce) were well correlated with HPLC data because the correlation coefficient (r) was equal to 0.99 in both comparisons (**Fig 4**). Vertical dashed lines in the linear regression analysis graphs indicate the maximal HPLC value found in our previous study. When considering eumelanins, r was equal to 0.83 and 0.91 for v(mi,ce) and n″(m,ce), respectively (**Fig 5*A***, ***B***). In the case of pheomelanins, the correlation coefficients were slightly better because r was equal to 0.92 and 0.93 in the case of v(mi,ce) and n″(m,ce), respectively (**Fig 5*C***, ***D***). The fact that one nevus cell line point fell very close to the melanoma cells group, however, makes these two r values less reliable than for total melanin or eumelanins (compare **Fig 5*C***, ***D*** with **Figs 4**, **5*A***, ***B***).

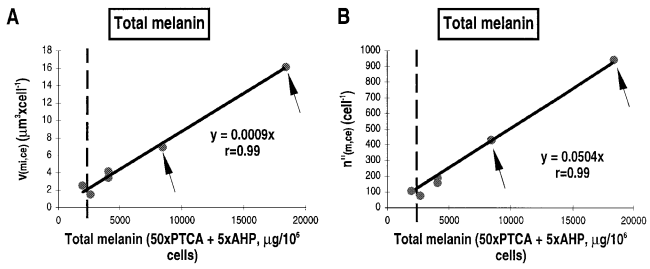

Figure 4. Linear regression analysis of HPLC and stereologic melanization data for total melanin by using the stereologic parameters v(mi,ce) (*A*) and n″(m,ce) (*B*). The vertical dashed line represents the maximal melanization level found by HPLC in our previous study in unstimulated melanoma cells. *Arrows* show LEA and CARA cells.

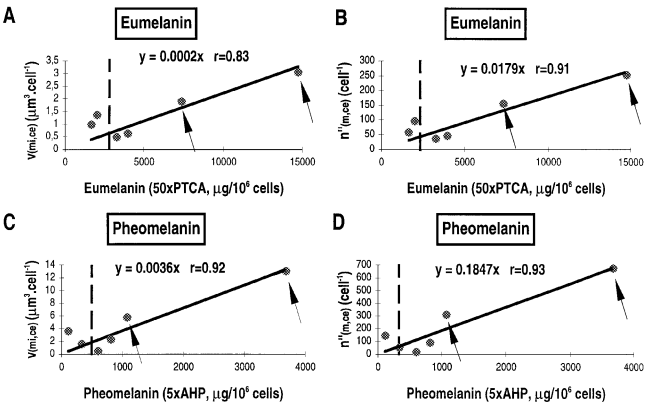

Figure 5. Linear regression analysis of HPLC and stereologic melanization data for eumelanin (*A* and *B*) and pheomelanin (*C* and *D*) by using the stereologic parameters v(mi,ce) (*A* and *C*) and n″(m,ce) (*B* and *D*). The vertical dashed line represents the maximal melanization level found by HPLC in our previous study in unstimulated melanoma cells. *Arrows* show LEA and CARA cells.

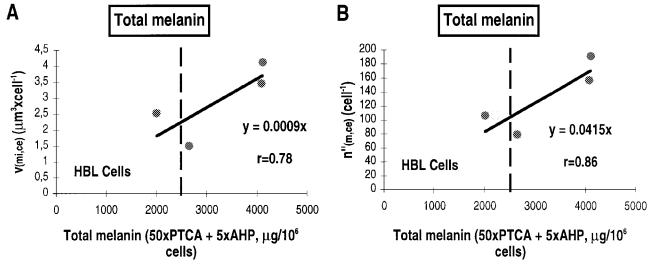

Figure 6. Linear regression analysis of HPLC and stereologic melanization data for total melanin by using the stereologic parameters v(mi,ce) (*A*) and n″(m,ce) (*B*) performed in stimulated HBL melanoma cells alone. The vertical dashed line represents the maximal melanization level found by HPLC in our previous study in unstimulated melanoma cells.

HBL melanoma cells alone When considering only HBL cells and total melanin, r was equal to 0.78 and 0.86 when using v(mi,ce) and n″(m,ce), respectively (**Fig 6*A*, *B***). The same parameters, however, were not correlated with HPLC data in the case of eumelanins or pheomelanins when using v(mi,ce) or n″(m,ce) (not shown). The same could not be accomplished for nevus cells because we had only two cell lines at our disposal.

Linear regression analyses between stereologic parameters for all the cell lines and experimental conditions When considering all the cell lines and experimental conditions, all the intracellular melanization parameters correlated well with each other and a(mi,m) was not correlated with intracellular melanization parameters, whatever the type of pigment (not shown). For this reason, v(mi,ce), n″(m,ce), and VV(mi,cy) always gave similar r values when compared with HPLC data by linear regression analysis for a given pigment.

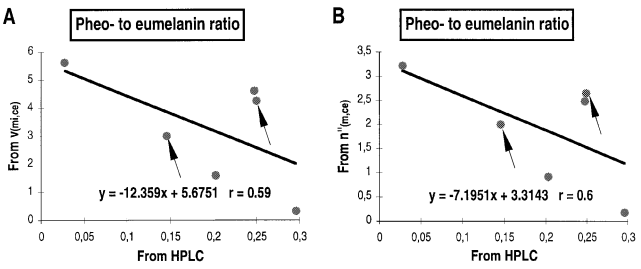

Figure 7. Linear regression analysis of the P/E ratios estimated from HPLC and stereologic data calculated from v(mi,ce) (*A*) and n″(m,ce) (*B*) for all the experimental conditions and cell lines. *Arrows* show LEA and CARA cells.

P/E ratio We also calculated the P/E ratio from stereologic and HPLC data. From stereology, two alternative calculations were performed and evaluated by utilizing the four following intracellular melanization parameters as eumelanins and pheomelanins data: v(mi,ce), n″(m,ce), A(mi,cp), and N(m,cp). This allowed us to evaluate eight P/E ratio estimators because of the two possible alternatives described in *Materials and Methods*. By using the second alternative (P/E estimated from the P and E values averaged over the S and B blocks), we obtained very moderate correlations because r was equal to 0.59, 0.6, 0.59, and 0.64 in the case of v(mi,ce) (**Fig 7*A***), n″(m,ce) (**Fig 7*B***), A(mi,cp) (not shown), and N(m,cp) (not shown), respectively. No correlation, however, was found when using the first alternative (mean of P/E ratios obtained in S and B blocks), whatever the initial stereologic parameter. Additionally, whatever the calculation method of the P/E ratio, linear regression analyses did not give any correlation when the $y = ax$ model was used (not shown). Moreover, whatever the stereologic P/E ratio or initial stereologic parameter, the slope of the $y = ax + b$ model was negative (**Fig 7**) when the expected slope should be positive.

It is also striking to note that both calculation alternatives for the P/E estimator correlated well with each other in this study: r was equal to 0.82, 0.8, 0.73, 0.74, and 0.93 ($r = 0.8 \pm 0.07$ $n = 5$) when VV(mi,cy), v(mi,ce), n″(m,ce), N(m,cp), and A(mi,cp) were used, respectively, and the average slope of the $y = ax$ linear regression model was close to 1 ($a = 1.45 \pm 0.2$) (not shown). Additionally, when suppressing one particularly aberrant point corresponding to the LEA nevus cell line, the r values and slopes of the $y = ax$ linear regression models were much more satisfactory ($r = 0.91 \pm 0.11$, $n = 5$ and $a = 1.23 \pm 0.18$, $n = 5$) (not shown). Similar regressions performed in our previous study (Donois *et al*, 1998b) gave no correlation between both P/E stereologic estimators (unpublished data), suggesting better quality eumelanin and pheomelanin stereologic data in this study.

DISCUSSION

In our preceding study, we performed similar comparisons in several melanoma cell lines cultured in basic Ham F10 medium with usual supplements (Donois *et al*, 1998b). The results of this study have shown good correlations between stereologic and HPLC data only in the case of total melanin. As a result, the P/E ratios were not correlated between both methods. Three hypotheses were then formulated (Donois *et al*, 1998b). Succinctly, the first involved the very low level of intracellular melanization inducing poor quality stereologic estimators. The second concerned the possible lack of specificity of the alkali elution method, particularly in melanoma cells, indirectly suggested by some authors (Ozeki *et al*, 1995, 1996). In effect, our modification of the original alkali elution method was validated in normal human follicular melanocytes corresponding to different hair types and is perhaps not valid in melanoma cells in which melanogenesis is strongly inhibited and potentially perturbed compared with normal human melanocytes. The third hypothesis implicates the possible bias in measuring only DHICA

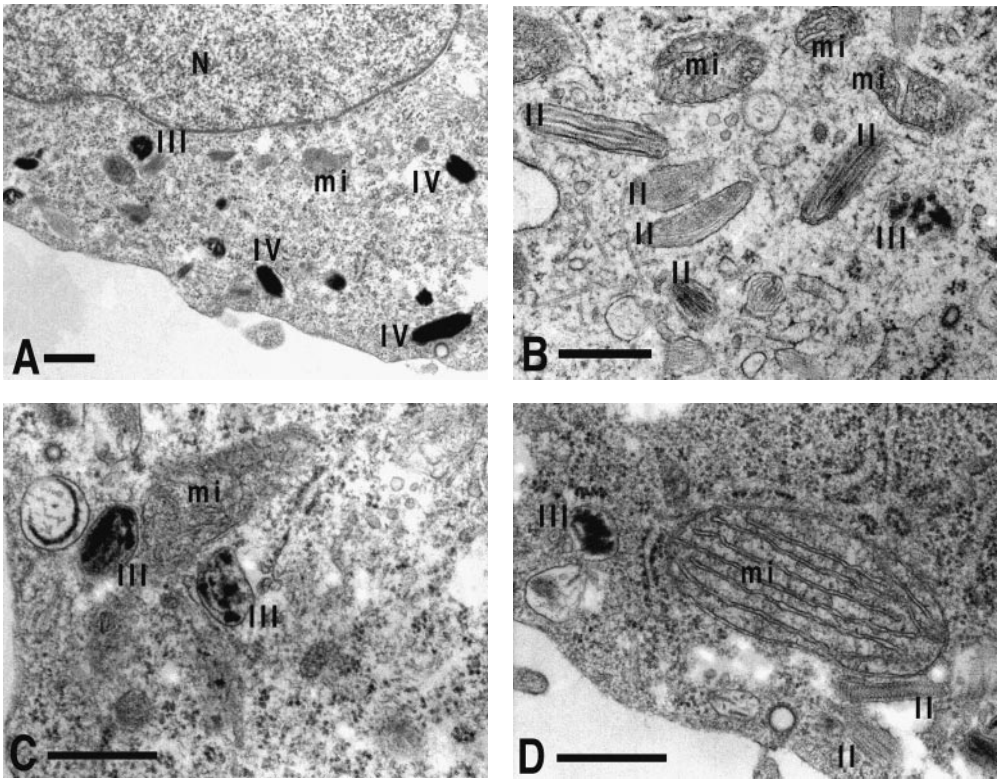

Figure 8. Ultrastructural features of melanosomes of HBL cells. I, II, III, IV, stage of maturation of melanosomes; mi, mitochondria; N, nucleus. (*A*) and (*B*), HBL cells cultured in 110/20.6 μM of Tyr/cysteine; (*C*) and (*D*), HBL cells cultured in 40/20.6 μM of Tyr/cysteine. *Scale bars*: 0.5 μm.

units (pyrrole-2,3,5-tricarboxylic acid) from the degraded eumelanin biopolymer, which could also induce a bias in the HPLC estimation of eumelanins and total melanin contents.

In this study, very different results were obtained because the stereologic and HPLC estimations of total melanin, eumelanins, and pheomelanins intracellular contents were well correlated when using all the six experimental points (melanoma and nevus cells) in a linear regression analysis, even though all the correlations were not significant (see below).

Statistical significance of the correlation coefficients The significance of the correlation between the different parameters studied was first assessed by using a parametric approach requiring a gaussian distribution of the variables which cannot be verified. The correlations were found significant at $p = 0.05$ for correlations illustrated in **Figs 4** and **5**, but not for correlations obtained from melanoma cells alone or from the P/E ratios, illustrated in **Figs 6** and **7**. When using a Kendall's nonparametric test, these correlations were significant for **Fig 4** but not for **Figs 5–7**.

Concerning the linear regression analysis between the intracellular melanization stereologic data, correlations were significant at $p = 0.05$ for each type of pigment and whatever the statistical test used (parametric or nonparametric).

The correlations between the two alternatives of calculation of the P/E ratio were significant at $p = 0.05$ for the source parameters VV(mi,cy) and A(mi,cp), were significant at $p = 0.1$ for the parameters v(mi,ce) and N(m,cp), and were not significant for n″(m,ce); however, these correlations were never significant, either at $p = 0.05$ or at $p = 0.1$, when using a Kendall's nonparametric test. Nevertheless, when suppressing one particularly aberrant point, these correlations were singificant at $p = 0.05$ whatever the statistical test used.

Even though our stereologic data were not systematically significantly correlated with HPLC data, essentially when nonparametric tests were used, it is clear that there is an emergence of correlation between our preceding study (Donois *et al*, 1998b) and this study, on which this discussion mainly relies.

The particular case of melanoma cells This confirms our first hypothesis, but when stimulated HBL melanoma cells alone were used for linear regression analyses (four points), a moderate and less reliable correlation was found in total melanin and no correlation was met for eumelanin and pheomelanin. This suggests that the second hypothesis involving the specificity of melanogenesis in melanoma cells with no specialized pheomelanosomes and eumelanosomes, and/or the first hypothesis involving a lack of sensitivity of our method for poorly melanized cells is (are) very likely.

The P/E ratios When considering the six points, it is also striking to note that the two alternatives in calculating the P/E stereologic estimators correlated well with each other in this study, whereas similar regression analysis performed in our previous study gave no correlation between these two P/E stereologic estimators (unpublished data). This lack of correlation between the P/E ratios of the first and second alternatives in our preceding study probably denotes an imprecision of the stereologic estimates of eumelanins and pheomelanins contents in unstimulated melanoma cells. The quality of the two stereologic P/E ratios was greatly improved in this study because both alternatives correlated well with each other with a slope close to 1. This suggests that it is not the stereologic sampling and calculations that are responsible for the low correlation between the HPLC and stereologic P/E ratios, but rather the lack of specificity of the alkali elution method, or the variable DHI/DHICA ratio and/or the imprecision of the stereologic method for poorly pigmented cells (i.e., melanoma cells and melanocyte profiles submitted to the alkali elution).

The ultrastructural aspect of melanosomes of the different cell lines and conditions is illustrated in **Figs 8** and **9**. Unfortunately, we did not obtain enough high magnification micrographs from the alkali-treated sections to enable us to reach a conclusion on this aspect.

In HBL melanoma cells, melanosomes were in the majority of the eumelanosome type from an ultrastructural angle (**Fig 8*A***, ***B***). Sometimes, mixed type melanosomes could be observed (elliptic in shape with filaments and a spotty pattern of melanin deposition) (**Fig 8*C***). Very few pheomelanosomes could be seen (**Fig 8*D***). No particular difference was noticed between the different experimental conditions for this cell line.

In LEA and CARA nevus cells, melanosomes were more numerous than in HBL cells and in a majority of the eumelanosome type (**Fig 9**). Excluding the stage II eumelanosomes, there was no evident difference of level of maturation with HBL cell melanosomes. Typical pheomelanosomes were rarely observed (**Fig 9*B***, ***C***).

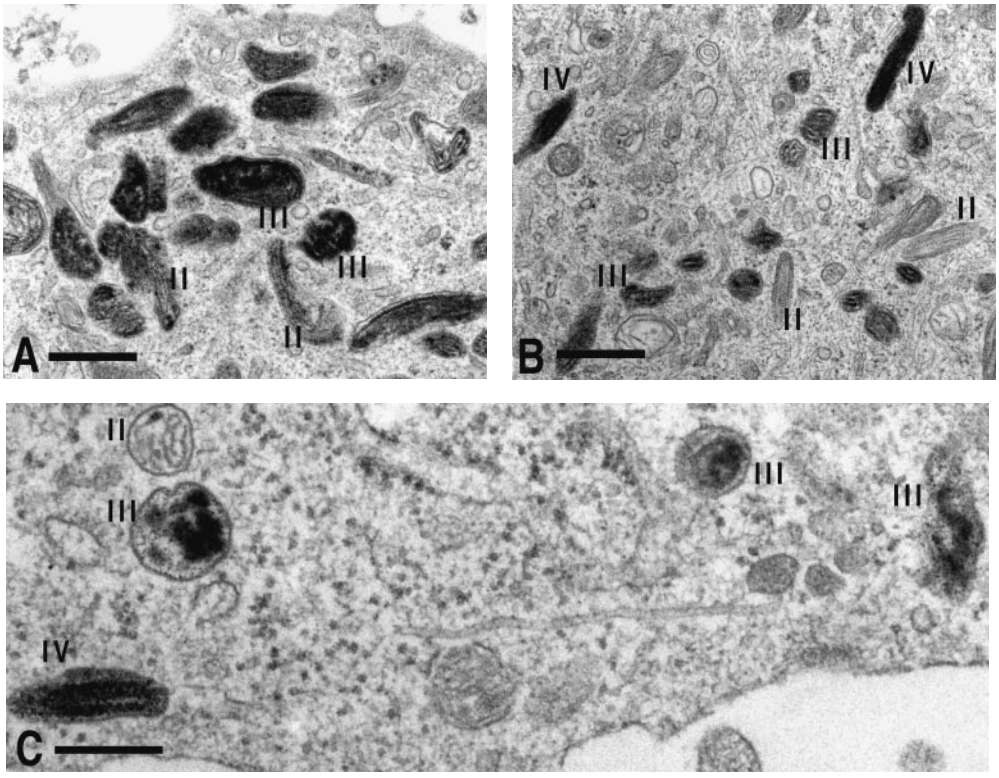

Figure 9. Ultrastructural features of melanosomes of LEA (*A, B*) and CARA (*C*) nevus cells. I, II, III, IV, stage of maturation of melanosomes; mi, mitochondria; N, nucleus. *Scale bars*: 0.5 μm.

In 1993, Inazu and Mishima demonstrated that in normal human follicular melanocytes, eumelanogenic and pheomelanogenic melanosomes are present in the same melanocytes and that they are characterized by an ellipsoidal and spheroidal shape, respectively (Inazu and Mishima, 1993). Besides, it is now well established that eumelanins and pheomelanins are present in human epidermis (Thody *et al*, 1991), that the P/E ratio varies as a function of the donor skin type and the source of the investigated sample (cultured melanocytes or skin samples) (Hunt *et al*, 1995a), and that, like in mouse hair follicles (Granholm and Van Amerongen, 1991), the P/E ratio can be modified by α-MSH or α-MSH superpotent analogs in cultured normal human epidermal melanocytes (Hunt *et al*, 1995b). In the mouse, the α-MSH superpotent analog-induced switch from pheomelanogenesis to eumelanogenesis is accompanied by an ultrastructural switch from circular to elliptic melanosomes (Granholm and Van Amerongen, 1991). If it is true that mixed melanins can be synthesized *in vitro* (Ito *et al*, 1980; Agrup *et al*, 1982) and that mixed (mosaic) melanosomes can be observed in human follicular and isolated murine melanocytes (Sato *et al*, 1985; Ortonne and Prota, 1993; Prota, 1993), there is no certainty that mixed melanins are deposited inside a given melanosome *in vivo*.

In fact, when a melanocytic cell line is found to show a mixed melanogenesis by HPLC it is impossible to determine whether this mixed melanogenesis takes place at the cellular or the organelle level. There are even more results indicating that mixed melanogenesis does not really exist, at least quantitatively. Effectively, Inazu and Mishima prove in 1993 that in human follicular melanocytes, pheomelanins and eumelanins are deposited in spherical and ellipsoidal melanosomes, respectively, and that both types of specialized melanosome can be found in the same melanocyte (Inazu and Mishima, 1993). Additionally, this last result is probably valid in human epidermal melanocytes because Nakagawa and Imokawa have shown that the E/P ratio based on an HPLC analysis is quite well correlated with the E/P ratio based on the ultrastructural phenotype of melanosomes (Nakagawa and Imokawa, 1996).

In melanoma cells, however, the condition is perhaps different as Ando *et al* have detected melanosomes with an incomplete solubilization pattern after alkali elution of ultrathin sections associated with aberrant morphologic aspect of most of the melanosomes observed (Ando *et al*, 1993). This suggests that in this pathologic context, mixed melanogenesis is possible. This incomplete pattern of solubilization has not yet been observed in our laboratory, neither in normal human epidermal or follicular melanocytes nor in melanoma cells (personal observation). For these reasons, it is reasonable to conceive very specialized melanosomes in normal human epidermal melanocytes; however, this must by clarified and our quantitative approach, applied to cultured human normal epidermal melanocytes, in combination with chemical methods, could contribute to answering this question.

Finally, the results of this study do not permit us to reach a definite conclusion about the third hypothesis related to the bias in measuring only DHICA units in eumelanins, even though it does not seem to be likely.

This work was supported by grants from the Fondation René Touraine (E.D.) and from the Fondation P. et T. Lefebvre (V.d.M. and G.G.). We would also like to thank Renato Morandini for managing cell culture experiments and Philippe Mersch and Isabelle Borsu for their very valuable technical assistance.

REFERENCES

Agrup G, Rorsman H, Hannson C, Rosengren E: The effect of cysteine on oxidation of tyrosine, dopa and cysteinyldopas. *Arch Dermatol Res* 272:103–115, 1982

Ando O, Mishima Y, Hanada S, Suemoto Y, Atobe J, Kurimoto M: Analyses of mixed melanogenesis in tyrosinase cDNA-transfected human amelanotic melanoma cells. *J Invest Dermatol* 101:864–870, 1993

Bolender RP: Biological stereology: history, present state, future directions. *Microsc Res Tech* 21:255–261, 1992

Bron C, Gremillet P, Launay D, Jourlin M, Gautschi HP, Bächi T, Schüpbach J: Three-dimensional electron microscopy of entire cells. *J Microsc* 157:115–126, 1990

Donois E, Freund O, Surlève-Bazeille J-E, Taïeb A: Stereological image analysis of human cultured melanocytes observed by transmission electron microscopy. *Microsc Res Tech* 36:188–200, 1997

Donois E, del Marmol V, Taïeb A, Ghanem G, Surlève-Bazeille J-E: A stereological image analysis method for the quantification of eu- and pheomelanin. *Anal Quant Cytol Histol* 1998a, in press

Donois E, del Marmol V, Wakamatsu K, Ito S, Ghanem G, Surlève-Bazeille J-E: Comparison of high performance liquid chromatography and stereological image analysis for the quantitation of eu- and pheomelanins in melanoma cells. *Pigment Cell Res* 11:86–93, 1998b

Granholm NH, Van Amerongen AW: Effects of exogenous MSH on the transformation from phaeo- to eumelanogenesis within C57BL/6J-A^y/a hairbulb melanocytes. *J Invest Dermatol* 96:78–84, 1991

Hunt G, Kyne S, Ito S, Wakamatsu K, Todd C, Thody AJ: Eumelanin and phaeomelanin

contents of human epidermis and cultured melanocytes. *Pigment Cell Res* 8:202–208, 1995a

Hunt G, Kyne S, Wakamatsu K, Ito S, Thody AJ: [Nle^4,D-Phe^7]-α-Melanocyte-Stimulating Hormone increases the Eumelanin:pheomelanin ratio in cultured human melanocytes. *J Invest Dermatol* 104:83–85, 1995b

Inazu M, Mishima Y: Detection of eumelanogenic and pheomelanogenic melanosomes in the same normal human melanocyte. *J Invest Dermatol* 100:172S–175S, 1993

Ito S: High-performance liquid chromatography (HPLC) analysis of eu- and pheomelanin in melanogenesis control. *J Invest Dermatol* 100:166S–171S, 1993

Ito S, Fujita K: Microanalysis of eumelanin and pheomelanin in hair and melanomas by chemical degradation and liquid chromatography. *Anal Biochem* 144:527–536, 1985

Ito S, Jimbow K: Quantitative analysis of eumelanin and pheomelanin in hair and melanomas. *J Invest Dermatol* 80:268–272, 1983

Ito S, Wakamatsu K: An improved modification of permanganate oxidation of eumelanin that gives a constant yield of pyrrole-2,3,5-tricarboxylic acid. *Pigment Cell Res* 7:141–144, 1994

Ito S, Novellino E, Chioccara F, Misuraca G, Prota G: Co-polymerization of dopa and cysteinyldopa in melanogenesis in vitro. *Experientia* 36:822–823, 1980

Jimbow K, Ishida O, Ito S, Hori Y, Witkop CJ, King RA: Combined chemical and electron microscopic studies of pheomelanosomes in human red hair. *J Invest Dermatol* 81:506–511, 1983

Jiménez-Cervantes C, Solano F, Kobayashi T, Urabe K, Hearing VJ, Lozano JA, Garcìa-Borròn JC: A new enzymatic function in the melanogenic pathway: the 5,6-dihydroxyindole-2-carboxylic acid oxidase activity of tyrosinase-related protein-1 (TRP-1). *J Biol Chem* 269:7993–8001, 1994

Kameyama K, Takemura T, Hamada Y, *et al*: Pigment production in murine melanoma cells is regulated by tyrosinase, tyrosinase-related protein 1 (TRP1), DOPAchrome tautomerase (TRP2), and a melanogenic inhibitor. *J Invest Dermatol* 100:126–131, 1993

Kobayashi T, Urabe K, Winder A, *et al*: Tyrosinase related protein 1 (TRP1) functions as a DHICA oxidase in melanin biosynthesis. *Embo J* 13:5818–5825, 1994

Leonard LJ, Townsend D, King RA: Function of dopachrome oxidoreductase and metal ions in dopachrome conversion in the eumelanin pathway. *Biochem* 27:6156–6159, 1988

del Marmol V, Ito S, Jackson I, *et al*: TRP-1 expression correlates with eumelanogenesis in human pigment cells in culture. *Febs Let* 327:307–310, 1993

del Marmol V, Ito S, Bouchard B, Libert A, Wakamatsu K, Ghanem G, Solano F: Cysteine deprivation promotes eumelanogenesis in human melanoma cells. *J Invest Dermatol* 107:698–702, 1996

Mayhew TM, White FH: Ultrastructural morphometry of isolated cells: methods, models and applications. *Path Res Pract* 166:239–259, 1980

Mishima Y: A post melanosomal era: control of melanogenesis and melanoma growth. In: Mishima Y (ed.). *XIVth International Pigment Cell Conference. The Pigment Cell: From the Molecular Level to the Clinical Level, Kobe, Japan*. Supplement, 2, 3–16. Munksgaard–Copenhagen, Pigment Cell Research, 1990

Nakagawa H, Imokawa G: Characterization of melanogenesis in normal human epidermal melanocytes by chemical and ultrastructural analysis. *Pigment Cell Res* 9:175–178, 1996

Napolitano A, Memoli S, Crescenzi O, Prota G: Oxidative polymerization of the pheomelanin precursor 5-hydroxy-1,4-benzothiazinylalanine: a new hint to the pigment structure. *J Org Chem* 61:598–604, 1996

Odh G, Hindemith A, Carstam R, Paulson J, Rosengren E, Rorsman H: Melanins in IGR1 Melanoma cells. *Pigment Cell Res* 7:419–427, 1994

Ortonne J-P, Prota G: Hair Melanins and hair color: ultrastructural and biochemical aspects. *J Invest Dermatol* 101:82S–89S, 1993

Ozeki H, Ito S, Wakamatsu K: Chemical characterization of melanins in sheep wool and human hair. *Pigment Cell Res* 9:51–57, 1996

Ozeki H, Ito S, Wakamatsu K, Hirobe T: Chemical characterization of hair melanins in various coat-color mutants of mice. *J Invest Dermatol* 105:361–366, 1995

Poole MC: An image processing/stereological analysis system for transmission electron microscopy. *Microsc Res Tech* 21:283–291, 1992

Prota G: Recent advance in the chemistry of melanogenesis in mammals. *J Invest Dermatol* 75:122–127, 1980

Prota G: Regulatory mechanisms of melanogenesis: Beyond the tyrosinase concept. *J Invest Dermatol* 100:156S–161S, 1993

Rawles ME: Origin of pigment cells from the neural crest in the mouse embryo. *Physiol Zool* 20:248–266, 1947

Sato C, Ito S, Takeuchi T: Establishement of a mouse melanocyte clone which synthesizes both eumelanin and pheomelanin. *Cell Struct Funct* 10:421–425, 1985

Schraermeyer U: The intracellular origin of the melanosome in pigment cells. A review of ultrastructural data. *Histol Histopathol* 11:445–462, 1996

Solano F, Jiménez-Cervantes C, Martínez-Liarte JH, García-Borrón JC, Jara JR, Lozano JA: Molecular mechanism for catalysis by a new zinc-enzyme, dopachrome tautomerase. *Biochem J* 313:447–453, 1996

Thody AJ, Higgins EM, Wakamatsu K, Ito S, Burchill SA, Marks JM: Pheomelanin as well as eumelanin is present in human epidermis. *J Invest Dermatol* 97:340–344, 1991

Wehrle-Haller B, Morrison-Graham K, Weston JA: Ectopic c-kit expression affects the fate of melanocyte precursors in *Patch* mutant embryos. *Dev Biol* 177:463–474, 1996

Weibel ER: Practical methods for biological morphometry. In: Parsons DF (ed.). *Stereological Methods*, Vol. 1. London: Academic Press, 1979

Weibel ER: Measuring through the microscope: development and evolution of stereological methods. *J Microsc* 155:393–403, 1989